DOI: 10.1021/ma102917u

Macromolecules
COMMUNICATION TO THE EDITOR

Mapping Polymer Phase Diagram in Nanoliter Droplets

Feng Shi,[†] Zuoyan Han,[†] Junfang Li,[†] Bo Zheng,*[,†] and Chi Wu[†,‡]

[†]*Department of Chemistry, The Chinese University of Hong Kong, Shatin, N.T., Hong Kong, China, and* [‡]*The Hefei National laboratory of Physical Science at Microscale, Department of Chemical Physics, The University of Science and Technology of China, Hefei, Anhui 230026, China*

Received December 21, 2010
Revised Manuscript Received January 13, 2011

Phase behavior captures an essential feature of classic thermodynamics. Because of the greater molecular size, polymer phase behavior possess unique aspects that make it significantly different from that of smaller molecules[1] and hence impressively enriches and extends the thermodynamic study.[2,3] Polymer phase diagrams, showing conditions under which polymer multiple phases can coexist at equilibrium, not only provide a basis to advance modern thermodynamics but also play an important role in polymer science and engineering, including, for instance, in the process of polymer preparation, purification, fractionation, and characterization.[1,4,5] Despite the widespread use of polymer phase diagrams, their construction in bulk scales has been restricted by two problems: the difficulty of obtaining narrowly distributed polymer samples in large quantity, and the long time required for the conventional phase transition measurement. Microfluidic systems provide an attractive platform to address these two problems by significantly reducing the consumption of reagents and the time for reaching thermal equilibrium. Previously, Mao et al. employed a linear temperature gradient to measure phase transition of polymer solutions in capillaries.[6] The technique was efficient in both time and sample consumption. However, the technique required preparation of the polymer solutions of different concentration beforehand, which usually required microliter volume of polymer solution or more and limited the throughput. To address this issue, several methods of concentrating polymer solution on-chip were developed to study protein crystallization[7] or phase transition of polymer solutions.[8,9] These methods were based on the water permeability in polydimethylsiloxane (PDMS), and the polymer solutions were concentrated on-chip through water evaporation through PDMS; therefore, the methods suffered from the long evaporation time to reach the desired concentrations. On the other hand, Hansen et al. developed microvalve integrated microdevices to efficiently generate a large number of nanoliter protein solution with different concentration and studied the phase diagram for protein crystallization.[10] The disadvantage of this method is the complicated design and operation of the microdevice. Laval et al. generated droplets on-chip with different concentration of adipic acid and studied the phase diagram.[11] The potential issue was the water evaporation through the PDMS chip, which limited the storage and measurement time. Herein, we use a droplet-based, PDMS/glass capillary composite microfluidic device[12] to rapidly produce an array of droplets containing polymer at various concentrations. The phase transition in the droplets of different polymer concentrations in a glass capillary can be quickly detected with a CCD camera or with eyes under a dark field microscope.

The droplet-based phase study consisted of two steps. In the first step, an array of nanoliter droplets of different polymer concentrations, separated and surrounded by a carrier fluid, was produced, transported, and stored inside a glass capillary (Figure 1a,b). We used a composite PDMS/glass capillary microfluidic device to conduct this step. The PDMS section of the composite device was used to form droplets of controllable polymer concentrations, and the coupled glass capillary was used to collect the droplets for the phase transition measurement. The PDMS chips had channels with $300 \times 300\ \mu m^2$ cross-sectional dimensions. Dispersed fluids (polymer solution and diluting agent) and carrier fluid were first loaded into the separate syringes; then the three fluids were injected into the PDMS microchannels via Teflon tubing by syringe pumps (Harvard Apparatus, PHD2000), with their flow rates being controlled by a Labview program. With the total flow rate of the dispersed fluids being kept constant, the volume of each dispersed fluid injected into a droplet is directly proportional to its respective volumetric flow rate at the time when the droplet is formed.[13] Therefore, polymer concentration in individual droplets can be controlled by varying the relative flow rates of the two dispersed fluids. After the droplets of desired concentrations were transported into the glass capillary, the flow was stopped and the capillary was disconnected, with its two ends being sealed with epoxy for further measurement.

In the second step, by utilizing the cloud point method, we detected the phase transition of the droplets inside the glass capillary with a dark-field microscope. In the cloud point method,[14] the polymer solution turns cloudy with sharp increase of scattered light intensity upon the phase transition point. In the current work, we monitored the phase transition of the droplets in the array at each given temperature. As each droplet represents one polymer concentration, we connected each phase transition *temperature* with its corresponding *composition* of each individual droplet, readily obtaining a temperature−composition phase diagram (Figure 1c).

The apparatus for the phase transition study consisted of a stereomicroscope (Leica, MZ16) in a dark field mode, a CCD camera (Diagnostic Instruments, SPOT Insight), and a home-built temperature controller, which was a copper block with built-in channels connected to a circulator (Julabo, F32-EH). The detection procedure was briefly outlined as follows: First, a mixture of powdered carbon black and PDMS precursor (Sylgard 184, Dow Corning) was spin-coated on the surface of the copper block to provide a black background. After the carbon black/PDMS thin layer was solidified, the glass capillary filled with the polymer droplets was placed on top of the carbon black/PDMS layer; meanwhile, the probe of a thermocouple meter (Sable Systems Internationals, TC-2000) was placed in the vicinity of the capillary to record the temperature. PDMS precursor without carbon black was then poured on top of the glass capillary, resulting in a covering layer of ca. 3 mm in thickness. The inherent properties in the PDMS precursor offer unique advantages for the resultant solid PDMS layer: (i) The covering PDMS layer covalently bonded to the background PDMS layer to form a uniform surrounding to identify the polymer droplets inside the glass capillary. (ii) The excellent optical transparency of PDMS facilitated the observation of the scattered light under the microscope. (iii) The top PDMS layer served as a thermal insulation to reduce the heat dissipation from the glass capillary

*To whom correspondence should be addressed. E-mail: bozheng@cuhk.edu.hk.

 Published on Web 01/27/2011

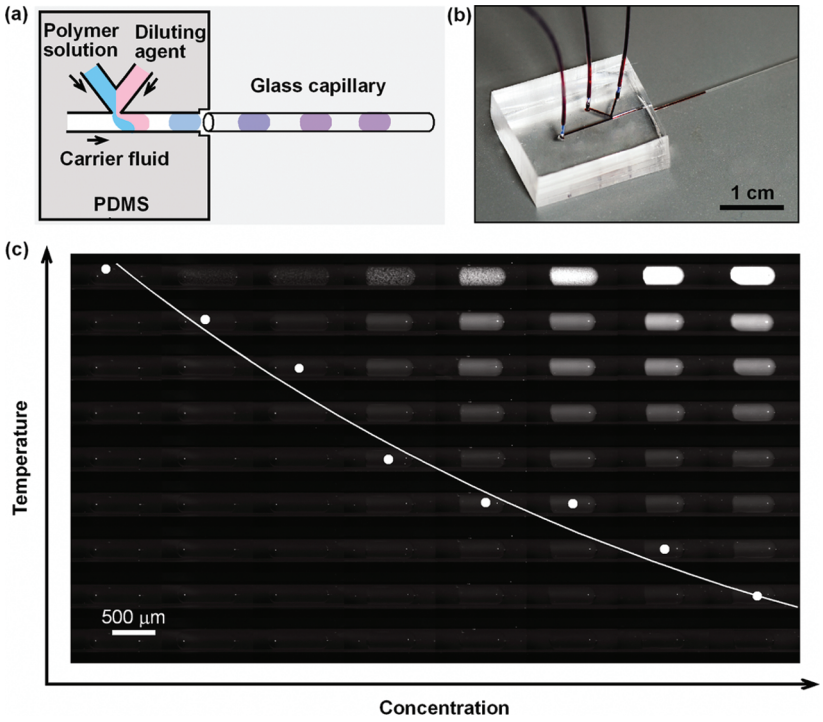

Figure 1. (a) Schematic illustration of the microfluidic setup of forming polymer droplets of various concentrations in a PDMS/glass capillary device. (b) A photograph of the composite device. All inlets and channels in the device are filled with $Fe(SCN)_3$ solution for clarity. (c) A microphotographic demonstration of mapping polymer phase diagram in droplets inside a glass capillary. The polymer solution in droplets is poly(*N*-isopropylacrylamide) (PNIPAM) (M_w = 2 400 000 g mol^{-1}) in water. Eight PNIPAM droplets of various concentrations are used for demonstration. The first turbid droplet of each concentration (marked by white dots) is connected, and a temperature−composition phase diagram curve is obtained.

to the environment. At each given temperature, images of droplets of different concentrations were taken in series with the CCD camera. Because of the fast heat transfer between the droplets with the copper block, the equilibrium time for a given temperature was very short (ca. 15 min). We were able to accomplish the detection of phase transition within 10 h.

We validated the droplet-based method by mapping the phase diagram of poly(*N*-isopropylacrylamide) (PNIPAM) in water. PNIPAM aqueous solution exhibits lower critical temperature miscibility;[15] that is, when heating, water molecules desorb from the hydrophobic portions; polymer chains collapse and aggregate; and then phase separation occurs.[16−18] The PNIPAM sample was synthesized via free radical polymerization and fractionated by using a mixture of acetone/hexane at room temperature.[19] Silicone oil (viscosity, 50 cP) served as the carrier fluid, offering an additional advantage that its similar refractive index (1.52) to glass (1.46) helped form a better background to identify the aqueous droplets inside the glass capillary. To ensure the formation and transportation of the aqueous PNIPAM droplets in microchannels, the inner wall of the PDMS/glass capillary microfluidic device was functionalized with 2% dichlorodimethylsilane in toluene. The flow rate of silicone oil was kept constant at 2.00 μL/min; the total flow rate of aqueous phases (PNIPAM solution and diluting agent) was maintained at 1.00 μL/min. Under the control of the Labview program, PNIPAM solution started at a flow rate of 0.05 μL/min with a ramp rate of 0.015 μL/min and ramp time of 59 s while the diluting agent (distilled water) started at a rate of 0.95 μL/min with a ramp rate of −0.015 μL/min.

The polymer concentration in each droplet was determined by using fluorescent internal marker. Fluorescein (ca. 10 μM) was added to the initial PNIPAM solution. In a separate experiment we confirmed that the presence of PNIPAM produced negligible difference in fluorescence signals of fluorescein, compared to a PNIPAM-free fluorescein solution. Figure 2a presents that in an array of 24 droplets produced by one run of the Labview program the PNIPAM concentration inside each droplet can be indicated by its corresponding droplet index. After precisely determining the PNIPAM concentration in each individual droplet, we detected the phase transition of the PNIPAM aqueous solution. The scattered light intensities of each individual droplet at various temperatures were measured by ImageJ (NIH). Figure 2b illustrates how the cloud point of one PNIPAM droplet is determined from the plot of scattered intensity versus temperature. We documented the cloud point of each indexed PNIPAM droplet and read its respective PNIPAM concentration in Figure 2a. The combination of the cloud point with its corresponding concentration readily resulted in a PNIPAM phase diagram within 20 h by using a few microliters of polymer solution.

We tested whether fluorescein affected the phase transition of PNIPAM solution. Two aqueous solutions of the same PNIPAM concentration were prepared, with one containing 10 μM fluorescein. The two solutions were separately loaded into two glass capillaries, and the ends of the capillaries were sealed with epoxy. By using the previous dark field setup, the phase transitions of the two solutions were studied in parallel. As shown in Figure 3, fluorescein has little effect on the phase transition of PNIPAM solution.

For comparison, we determined the phase transition of PNIPAM in water by using laser light scattering (LLS) as well. Details of LLS instrumentation can be found elsewhere.[20] Briefly, a series of PNIPAM aqueous solutions were prepared; for each concentration at various temperatures, the scattered light intensities at the scattering angle of 90° were recorded, and the phase transition of each concentration was measured one by one. The cloud point of each concentration was determined in a similar way as droplet-based microfluidic method.

The similarity and small discrepancy of the two curves from two methods (Figure 4) demonstrated it was feasible and reliable to determine polymer phase diagram using droplet-based

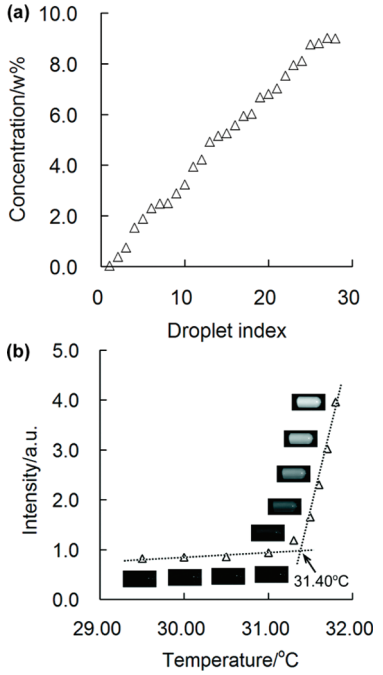

Figure 2. (a) PNIPAM (M_w = 478 000 g mol^{-1}) concentration inside a droplet in the droplet array closely corresponds with its droplet index. Various PNIPAM concentrations are designed and produced by the Labview program and accurately determined by measuring the fluorescence intensity from the internal marker of fluorescein. (b) Determination of the cloud point. Microphotographs show appearance evolution of one PNIPAM droplet (taken from those in Figure 1c) under a dark field microscope in the temperature range of phase transition. Upon phase transition occurring, microscopic heterogeneity in the PNIPAM droplets results in an intensity jump of scattered light.

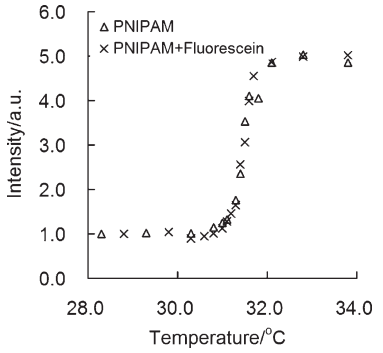

Figure 3. Effect of fluorescein on the phase transition of PNIPAM aqueous solution (M_w = 2 400 000 g mol^{-1}, C_{PNIPAM} = 1.14 wt %, and $C_{fluorescein}$ = 10 μM) is checked with a dark field microscope, by similarly measuring the scattered light intensity over the phase transition temperature range for the samples with (×) or without (Δ) fluorescein. The fluorescein-containing PNIPAM solution produces negligible difference in the scattering signals and therefore the cloud point, compared to the fluorescein-free solution of the same PNIPAM concentration.

microfluidic system. The temperature difference of the two methods (ca. 0.5 °C) was mainly due to the lower sensitivity of light detection by the CCD camera in the dark field microscope.

The droplets containing the PNIPAM solution were separated from the capillary wall by a thin layer of silicone oil.[12] The droplets were about 200 μm in diameter and 550 μm in length and presented large ratio of surface area to volume (S/V). The larger S/V ratio enhanced adsorption of PNIPAM to the water/oil interface, which could change the phase transition behavior and also cause uneven distribution of the scattering light intensity

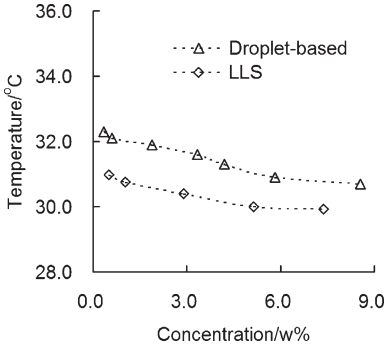

Figure 4. Comparison of phase diagram of PNIPAM (M_w = 478 000 g mol^{-1}, M_w/M_n = 1.11) in water constructed by droplet-based microfluidic system (Δ) and by laser light scattering (LLS) (◇).

across the droplets. Previous research on silicone oil emulsion in PNIPAM aqueous solution showed that the adsorption of PNIPAM onto the silicone water/oil interface decreased the PNIPAM concentration by less than 0.15%, while the volume ratio of silicone oil to water was 1:2.[21] In the current experiment, the volume ratio of silicone oil to water was about 1:1, and the PNIPAM concentration was at similar level to that in the previous research. In the experiment no obvious adsorption of the PNIPAM molecules was observed according to the scattering light intensity across the droplets (Figure 1c). Therefore, we conclude that the effect of the adsorption of PNIPAM onto the water/oil interface in the current system was negligible. In the case of significant adsorption, appropriate surfactants can be employed to prevent the adsorption of the molecules onto the interface.[22]

The droplet-based method has the following attractive features: (i) Only a few microliters of sample solution is needed to map the phase diagram. (ii) A polymer phase diagram can be accomplished within 20 h, benefiting from the vastly reduced thermal equilibrium time and simultaneous phase behavior measurement of different concentrations at each given temperature. (iii) The method is simple and straightforward. A series of various sample concentrations can be prepared in a few minutes in one step. This method can be applied to not only aqueous polymer solutions but also nonaqueous polymer solutions as long as the trace amount of fluorescent probe does not affect the phase transition. In the case where the liquid is noncompatible with PDMS,[23] the PDMS microchannel coated with a protection layer[24] or microchannels fabricated with the materials compatible with the liquid can be used.[25]

Acknowledgment. The financial support of the Chinese University of Hong Kong (Direct Grant 2060373), the Hong Kong Special Administration Region Earmarked Grants (404207 and 404209), and the National Natural Scientific Foundation of China Projects (20934005) is gratefully acknowledged.

References and Notes

(1) Koningsveld, R.; Stockmayer, W. H.; Nies, E. *Polymer Phase Diagrams: A Textbook*; Oxford University Press: New York, 2001.
(2) Chollakup, R.; Smitthipong, W.; Eisenbach, C. D.; Tirrell, M. *Macromolecules* **2010**, *43*, 2518–2528.
(3) Theodorakis, P. E.; Paul, W.; Binder, K. *Macromolecules* **2010**, *43*, 5137–5148.
(4) Koningsveld, R.; Kleintjens, L. A.; Geerissen, H.; Schuetzeichel, P.; Wolf, B. A. *Comperhensive Polymer Science: The Synthesis, Characterization, Reactions & Applications of Polymers*; Pergamon Press: New York, 1989.
(5) Wild, L. *Adv. Polym. Sci.* **1991**, *98*, 1–47.
(6) Mao, H. B.; Li, C. M.; Zhang, Y. J.; Bergbreiter, D. E.; Cremer, P. S. *J. Am. Chem. Soc.* **2003**, *125*, 2850–2851.

(7) Shim, J. U.; Cristobal, G.; Link, D. R.; Thorsen, T.; Jia, Y. W.; Piattelli, K.; Fraden, S. *J. Am. Chem. Soc.* **2007**, *129*, 8825–8835.
(8) Moreau, P.; Dehmoune, J.; Salmon, J.-B.; Leng, J. *Appl. Phys. Lett.* **2009**, *95*, 033108.
(9) Zhou, X. C.; Li, J. F.; Wu, C.; Zheng, B. *Macromol. Rapid Commun.* **2008**, *29*, 1363–1367.
(10) Hansen, C. L.; Sommer, M. O. A.; Quake, S. R. *Proc. Natl. Acad. Sci. U.S.A.* **2004**, *101*, 14431–14436.
(11) Laval, P.; Lisai, N.; Salmon, J.-B.; Joanicot, M. *Lab Chip* **2007**, *7*, 829–834.
(12) Zheng, B.; Tice, J. D.; Roach, L. S.; Ismagilov, R. F. *Angew. Chem., Int. Ed.* **2004**, *43*, 2508–2511.
(13) Zheng, B.; Roach, L. S.; Ismagilov, R. F. *J. Am. Chem. Soc.* **2003**, *125*, 11170–11171.
(14) Teraoka, I. *Polymer Solutions: An Introduction to Physical Properties*; Wiley: New York, 2002.
(15) Schild, H. G. *Prog. Polym. Sci.* **1992**, *17*, 163–249.
(16) Kubota, K.; Fujishige, S.; Ando, I. *J. Phys. Chem.* **1990**, *94*, 5154–5158.
(17) Wang, X. H.; Qiu, X. P.; Wu, C. *Macromolecules* **1998**, *31*, 2972–2976.
(18) Tiktopulo, E. I.; Uversky, V. N.; Lushchik, V. B.; Klenin, S. I.; Bychkova, V. E.; Ptitsyn, O. B. *Macromolecules* **1995**, *28*, 7519–7524.
(19) Wu, C.; Zhou, S. *Macromolecules* **1995**, *28*, 8381–8387.
(20) Wu, C.; Woo, K. F.; Luo, X. L.; Ma, D. Z. *Macromolecules* **1994**, *27*, 6055–6060.
(21) Ozawa, K.; Nomura, S.; Kawaguchi, M. *Colloids Surf., A* **2007**, *311*, 154–160.
(22) Roach, L. S.; Song, H.; Ismagilov, R. F. *Anal. Chem.* **2004**, *77*, 785–796.
(23) Lee, J. N.; Park, C.; Whitesides, G. M. *Anal. Chem.* **2003**, *75*, 6544–6554.
(24) Abate, A. R.; Lee, D.; Do, T.; Holtze, C.; Weitz, D. A. *Lab Chip* **2008**, *8*, 516–518.
(25) Rolland, J. P.; Van Dam, R. M.; Schorzman, D. A.; Quake, S. R.; DeSimone, J. M. *J. Am. Chem. Soc.* **2004**, *126*, 2322 2323.